Proceedings of the Eighteenth International Conference on
Civil, Structural and Environmental Engineering Computing
Edited by: P. Iványi, J. Kruis and B.H.V. Topping
Civil-Comp Conferences, Volume 10, Paper 2.6
Civil-Comp Press, Edinburgh, United Kingdom, 2025
ISSN: 2753-3239, doi: 10.4203/ccc.10.2.6

A New Algorithm To Determine Critical Speeds on Ballasted High-Speed Railway Bridges

G. Ferreira[1], P. A. Montenegro[1], A. A. Henriques[2] and R. Calçada[1]

[1] CONSTRUCT-iRAIL, Faculty of Engineering, University of Porto, Portugal
[2] CONSTRUCT-LABEST, Faculty of Engineering, University of Porto, Portugal

Abstract

Like all structures, it is impossible to characterize a bridge in a definitive manner. The intrinsic variability of materials, actions and building processes introduces mechanical and geometrical uncertainties. The study of structural safety, assessed through the relation between actions and bearing capacity, is as challenging as the variability of those parameters. One of the limits the Eurocodes impose on high-speed ballasted track railway bridges is verifying vertical deck acceleration. However, the apparently arbitrary origin of the normative limit has been discussed in recent years. To study this problem, it is necessary to address situations where the probabilities of failure are lower than 10e-4, which comes at a significant computational cost, especially considering multiple load models and possible critical speeds. A new algorithm is proposed based on subset simulation to find those speeds. An optimization study of the algorithm's parameters is presented. This process to determine critical speeds reduces the computational expense by three orders of magnitude that a more traditional Monte Carlo simulation would entail.

Keywords: railway bridges, high-speed railways, subset simulation, ballasted track, Eurocodes, probabilistic analysis

1 Introduction

High-speed railway bridges are prone to experience dynamic effects due to the repetitive nature of trains' axle loads. Ultimately, these actions can compromise materials' fatigue capacity, jeopardize track stability, or even be a cause of derailment. To contain such effects, the EN 1990 [1] provides limits to the allowable vertical deck acceleration. For ballasted track bridges, this limit is 3.5 m/s^2, a value that originates in studies by the European Rail Research Institute [2] that found ballast instability for accelerations of 7 m/s^2. Other authors note the seemingly arbitrary adoption of a safety factor of 2 [3].

Revising this normative limit is a key research topic highlighted by the European Union Agency for Railways [4]. Since the suitability of different limits should be based on newly proposed safety factors, a probabilistic assessment problem is constituted. However, considering that the acceptable probabilities of failure are usually in the 10^{-4} range, typical Monte Carlo simulation can become unfeasible regarding computational expense. To circumvent this limitation, the algorithm proposed in this communication uses subset simulation and a set of search cycle instructions to reduce significantly the necessary sample sizes.

2 Methods

2.1 Definitions

The present work concerns the study of vertical deck acceleration a. The failure event being considered is the surpassing of the strict physical value a_{Rl} of 7.0 m/s^2. Using definitions from the Joint Committee for Structural Safety [5], the target probability of failure is set at 10^{-4}, which is in accordance with values found in the literature [6, 7]. The probability of failure p_f is defined as:

$$p_f = P\left(a \geq a_{Rl}\right) \tag{1}$$

A critical speed is defined, for a given load model, as the lowest speed that results in:

$$p_f \geq 10^{-4} \tag{2}$$

The High-Speed Load Model (HSLM-A), which is given in the EN 1991-2 [8] as a set of 10 configurations of axle loads and spacings, is used for loading. Critical speeds $v_{crit,i}$ can be calculated for each of the 10 HSLM-A for a given bridge. The critical speed v_{crit} is therefore obtained with:

$$v_{crit} = \min\left(\{v_{crit,i}\}_{i=1}^{10}\right) \tag{3}$$

2.2 Subset simulation application basics

Subset simulation [9] uses conditional probability to estimate p_f as:

$$p_f = P(F_i) \prod_{i=1}^{m-1} P(F_{i+1}|F_i) \tag{4}$$

where F_i are m number of intermediate events (or levels) such that $F_1 \supset F_2 \supset \dots F_m$. For the first level, $P(F_1)$ is estimated with a crude Monte Carlo simulation, provided a reasonable N. The resulting acceleration values are ordered from highest (belonging to F_1) to lowest (farthest from F_1), as illustrated in Fig. 1a. Given a selected arbitrary intermediate probability p_0, the $(p_0 \times N)$-th value is classified as the cut-off y^*. The states of the random variables corresponding to values greater than or equal to y^* are used as generators (x) to generate the sample of the next level $(\tilde{x})$, using the Modified Metropolis Algorithm (MMA) [10]. This ensures that the states of the variables of the resulting sample are inside F_1. In the example in Fig. 1b, it is visible that every result in $i = 2$ is greater or equal to the cut-off that defines F_1. The process is repeated (Fig. 1c and Fig. 1d) until y^* is found inside F_m (i.e., $P(F_i) > p_0$). With $p_0 = 0.1$, probabilities of the order of magnitude of $10^{-4} = 0.1 \times 0.1 \times 0.1 \times 0.1$ are attainable with four levels ($F_m = F_4$). Note that in Fig. 1d, with $p_0 = 10$ and $N = 100$, $y*$ is in the 10th ordered position. Since in that example there are 13 results equal or greater than $y*$, $P(F_4) = 13/100 = 0.13 > p_0$, and as such, $p_f = 0.13 \prod_{i=1}^{4-1} 0.1 = 1.3 \times 10^{-4}$.

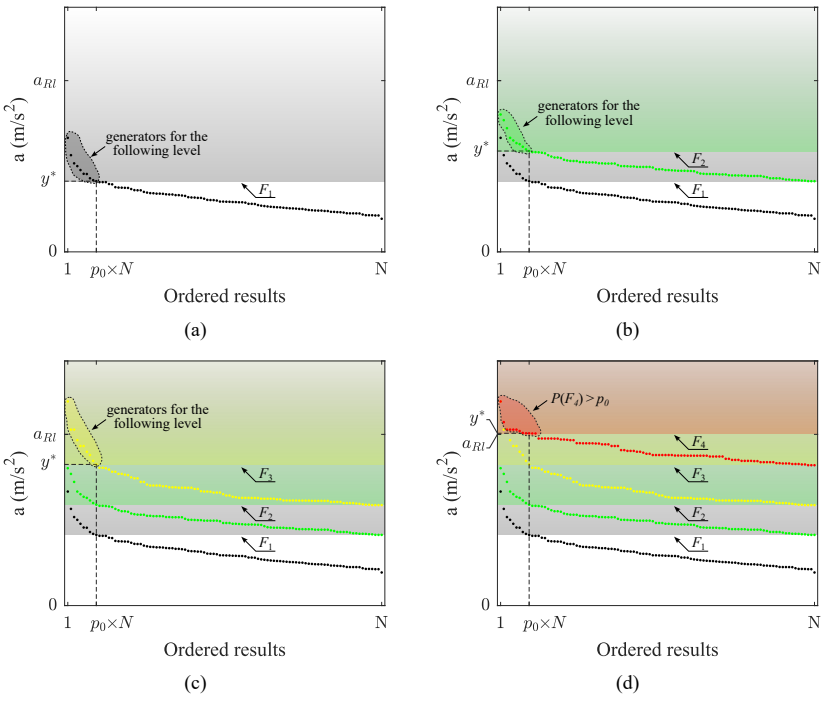

Figure 1: Visualization of subset simulation. (a) $i = 1$; (b) $i = 2$; (c) $i = 3$; (d) $i = 4$.

The diagram in Fig. 2 illustrates how subset simulation is applied in practice for this study. Initially, the random variables are sampled using MATLAB® [11] and combined with existing constant quantities to create the input for the FE model, which is designed in ANSYS® [12]. The dynamic response is calculated for the desired load model (i.e. one of the 10 HSLM-A configurations) using the Single Load Linear Superposition method [13]. It is then filtered with a low-pass Type II Chebyshev filter, cut off at 60 Hz, and the maximum absolute acceleration is stored for each randomly generated bridge. After this crude Monte Carlo phase, if no stopping criterion is met, the level counter is increased, and the ordered results greater or equal to y^* are used as the seeds for the Markov Chain Monte Carlo (MCMC). The MMA implementation is based on the work by Uribe [14]. In this work, the adopted proposal Probability Density Functions to obtain candidates η from the current state of a variable x_k are, for Gaussian distributed variables $N(\mu, \sigma^2)$:

$$\eta \sim N\left(x_k, \sigma^2\right) \tag{5}$$

and for uniformly distributed variables $U(a, b)$:

$$\eta \sim N\left(x_k, \frac{(b-a)^2}{12}\right) \tag{6}$$

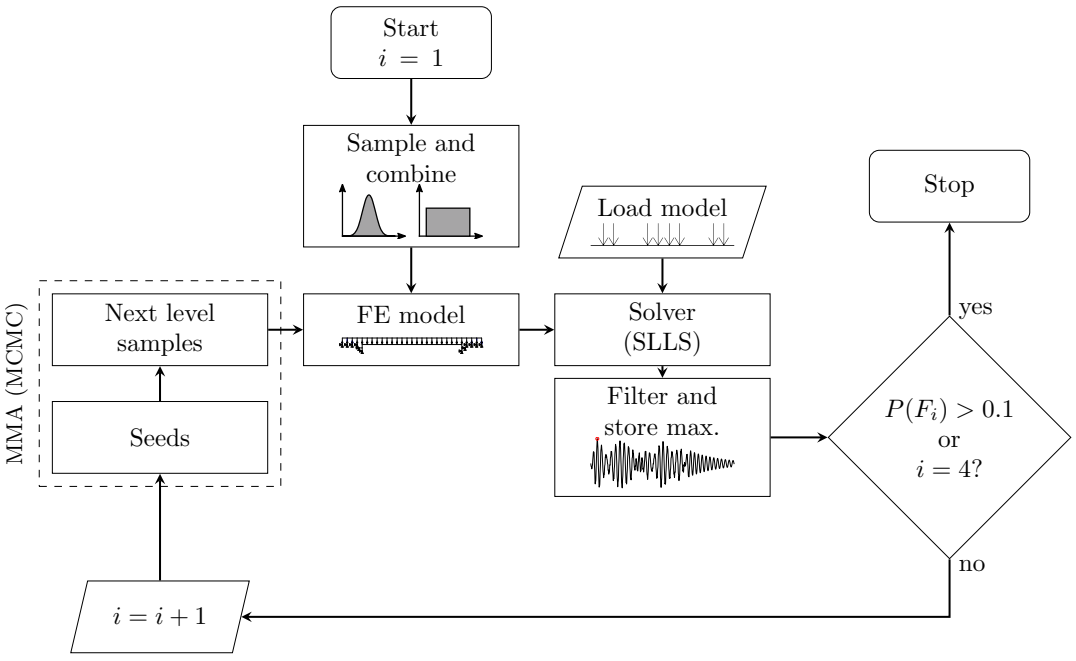

Figure 2: Application of subset simulation.

With the samples of the next level, new FE models are obtained, and the dynamic responses for the new set are calculated. The process stops after the $P(F_i) > 0.1$

condition occurs (after which p_f can be estimated) or if $i = 4$ (i.e., if the subset simulation is already in the fourth level, any possible p_f would be lower than 10^{-4}, and therefore not worthy of further exploration for this work). If $i \leq 4$, p_f is given by:

$$p_f = (p_0)^{i-1} \times P(F_i) \tag{7}$$

2.3 Proposed algorithm

Although the application of subset simulation is associated with considerable savings in computation time, this only applies to the estimation of probabilities for a given running speed. The question remains for which speed or set of speeds the probabilities must be calculated. Simulating coarse intervals of 10 km/h is incompatible with the sensitivity of most dynamic calculations concerning speed. Conversely, a finer 1 km/h interval is not feasible given all the possible values in a usual speed interval.

Hence, the algorithm summarized in Fig. 3 is introduced. The objective of this procedure is to avoid wasting computational resources that would be misused by calculating probabilities of failure lower than 10^{-5}. When the search cycle is initialized, the running speed v is set to its initial value (the lowest in the given speed range). After the initial analysis (i.e. the crude Monte Carlo simulation in $i = 1$), if the cut-off y^* is lower than a chosen threshold value y_t, the speed is increased to the next value. Note that y_t must be chosen appropriately so that exceeding it represents a substantial likelihood that p_f is near 10^{-4}. Initially, the speed increment is a coarse interval of 20 km/h. The cycle continues until the $y^* > y_t$ condition is satisfied. If the resulting p_f is greater than 10^{-4}, a finer speed cycle of 1 km/h increments is triggered, symbolized by the flag $\boxed{\text{F}}$. The running speed returns to the value immediately after the second-highest calculated speed ($v = v - 19$ km/h), and the cycle continues. During this phase, if $y^* < y_t$, flag $\boxed{\text{D}}$ is activated to store the information that at least one running speed was discarded during the finer cycle. The first time a $p_f > 10^{-4}$ is found, the current v is classified as a suitable candidate. If $\boxed{\text{D}}$ is off, no previous speed was discarded in $F1$ (i.e., the speed or speeds immediately before were calculated but turned out to be in the magnitude of 10^{-5} or lower), and the candidate is immediately accepted as v_{crit}. Otherwise, a $v = v - 1$ reverse search cycle is activated to check the previously discarded speed value until v_{crit} is confirmed.

2.4 Parameters for optimization

For the proposed algorithm to be viable regarding computational savings, the N, p_0, and y_t parameters must be set appropriately. Unoptimized parameters may lead to inefficient use of simulation capacity due to unnecessary time spent calculating v_{crit} candidates that result in $p_f \approx 0$ due to an increased amount of entries in the $v = v - 1$ reverse search cycle or due to insufficient dispersion in $i = 1$ results that jeopardizes further levels. Hence, a sensitivity study is performed to set appropriate parameters. The metrics adopted are the time required to go from v=140 km/h to v_{crit} and the total sample size n_S required for the simulation.

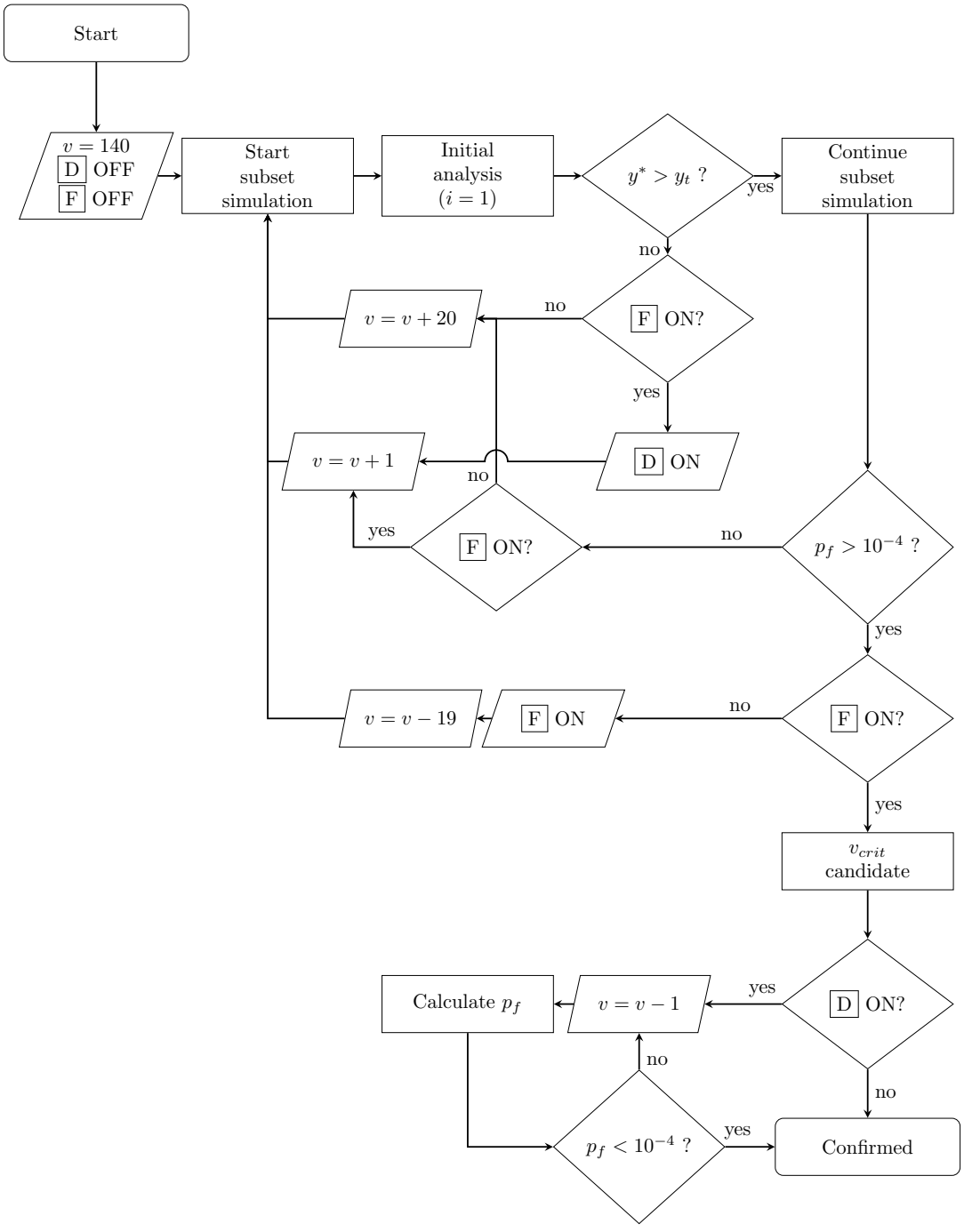

Figure 3: Algorithm to assess critical speed.

3 Results

3.1 Case study bridge

The example structure employed in this work is a single simply supported 12 m span of the Canelas bridge [6, 15], located in the Northern Line of the Portuguese Rail Network. Its deck has a cross-section of 4.5×0.7 m^2, embedded with HEB500 steel profiles. The ballasted track carries UIC60 rails, and neoprene bearings support the deck. The finite elements model is presented schematically in Fig. 4, where the constituting random variables are taken from [16].

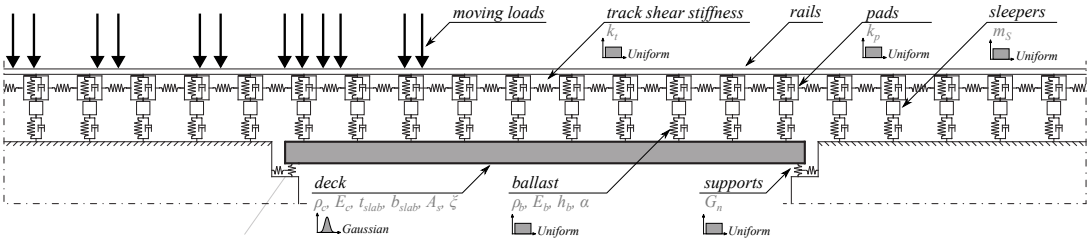

Figure 4: Schematic representation of the finite element model and random variables.

3.2 Complete run example

An example of a complete algorithm run is depicted in Fig. 5 (in the graphics, the offset in the coloured dots is meant to improve clarity and does not denote a change in speed). In this case, the sample size N for each level is 100 and $p_0 = 0.1$, which means that in the sorted results, y^* is in the $100 \times 0.1 = 10$-th position. In simulations 1 to 7, y^* was lower than y_t (3 m/s^2 in this case), meaning no simulation progressed beyond $i = 1$. In simulation 8, y^* is greater than y_t, causing the simulation to continue, resulting in a calculated p_f of 0.02. This result at 280 km/h initiates the finer speed increment cycle at 280-19=261 km/h. Simulations 9, 10 and 11 (261 km/h, 262 km/h, and 263 km/h, respectively) do not meet the y_t criterion. Simulation 12, at 264 km/h meets the criterion and returns $p_f = 5.1 \times 10^{-4}$, making it a suitable v_{crit} candidate. However, since there was at least one discarded speed, the algorithm runs simulation 13 at 263 km/h by fetching the stored $i = 1$ results and resuming the subset simulation. The resulting p_f is 1.2×10^{-4}, making this speed the new v_{crit} candidate. Simulation 14, at 262 km/h is also resumed, resulting in $p_f = 4 \times 10^{-5}$, confirming that 263 km/h as v_{crit} and finishing the algorithm run. It is worth noting that this application of the algorithm, with its iterative nature, allowed a critical speed to be found with a total sample size of 2,200 (100 per level, with a maximum of 400 per speed value). In contrast, running a similar procedure using crude Monte Carlo simulations would require a total sample size of over 1 million.

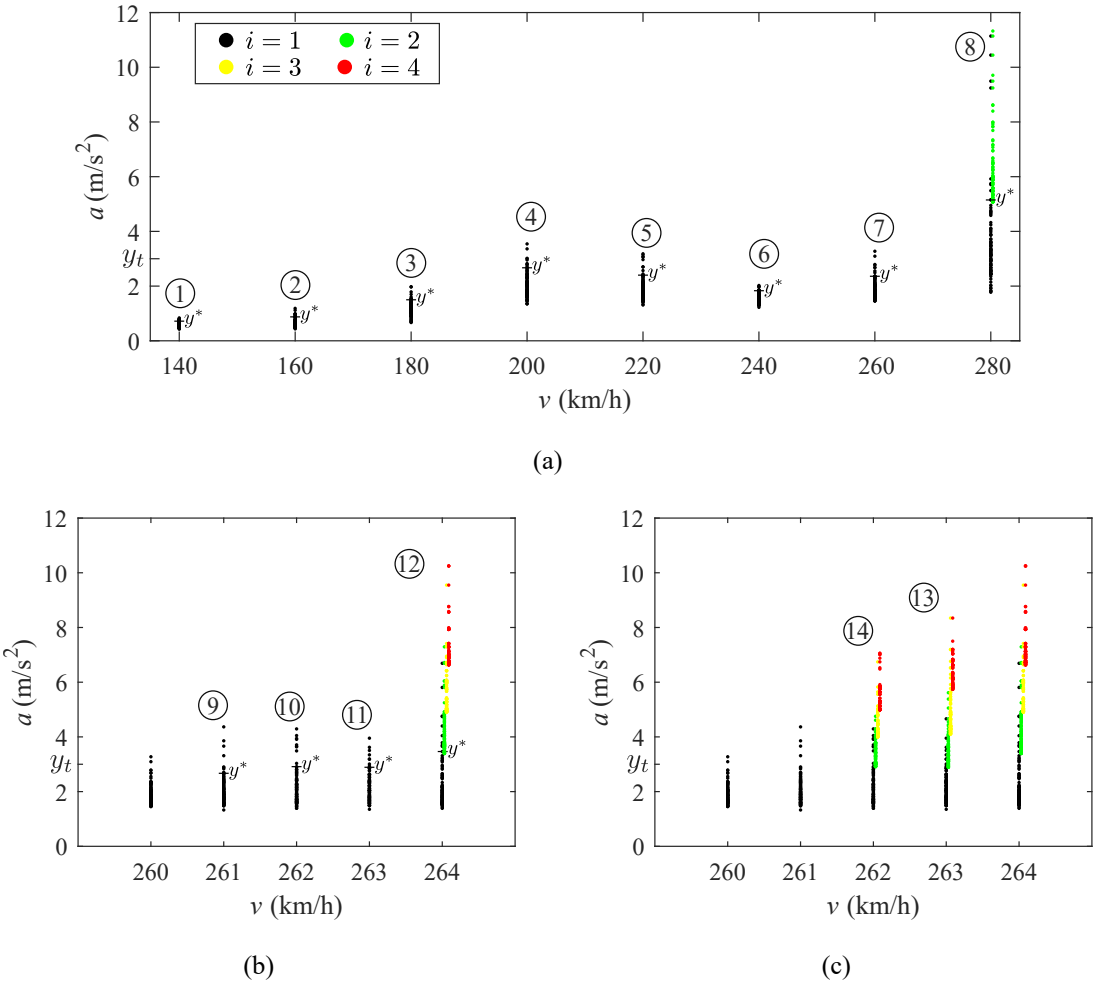

Figure 5: Example results from the application of the proposed algorithm. (a) Simulations 1 to 8; (b) simulations 9 to 12 (finer speed increment cycle); (c) simulations 13 and 14 ($v = v - 1$ reverse search cycle).

3.3 Optimization results

The HSLM-A3 train is used to perform the optimization study of the critical speed algorithm. The first parameter to be studied was the threshold value y_t in $i = 1$, which controls whether a speed value is discarded. For this part of the study, the sample size and the intermediate probability were fixed at $N = 100$ and $p_0 = 0.1$, and y_t varied between 2.0 m/s^2, 2.5 m/s^2, 3.0 m/s^2 and 3.5 m/s^2. Table 1 lists the time and total sample size needed to complete the algorithm and the resulting v_{crit}. It can be seen that using the values of 3.0 m/s^2 and 3.5 m/s^2 resulted in the least computational expense. However, further analysis of the simulation results revealed that the stricter 3.5 m/s^2 limit caused the algorithm to skip $v = 264$ km/h, which would have produced a suitable p_f and therefore a lower (and valid) v_{crit} candidate. Conversely, while it is true that using lower threshold values prevents prematurely

discarding of candidate speeds, this option also leads to increased time expenditure, as additional time is spent calculating candidates that are far from the final one. The threshold value $y_t = 3.0$ m/s^2 is henceforth kept as optimal.

y_t	2.0 m/s^2	2.5 m/s^2	3.0 m/s^2	3.5 m/s^2
time (h)	3:34	2:58	1:48	1:37
n_S	4200	3400	2200	2100
v_{crit} (km/h)	266	264	263	267

Table 1: Variation of the first level threshold y_t (HSLM-A3, $p_0 = 0.1$, $N = 100$).

The parametric analyses' results can be further illustrated by comparing the complementary Cumulative Distribution Function (CDF) of a simulation corresponding to a critical speed to the complementary CDF of its equivalent Monte Carlo simulation with $N = 100000$ (per [17]), as shown in Fig. 6. In the figures, the circles highlight the acceleration value (i.e., that simulation's y^* values) at the intermediate level, while the asterisk indicates the final calculated p_f. It can be seen that there is a close correspondence for the scenarios with y_t=2.5 m/s^2 and y_t=3.0 m/s^2, where not only is the calculated p_f in the same vicinity (of 10^{-4}), but the intermediate levels also follow the trend of the corresponding Monte Carlo simulation.

Using the aforementioned y_t value and a fixed sample size $N = 100$, the optimal intermediate probability is examined by varying p_0 between 0.05, 0.1 and 0.2. As shown in Table 2, adopting an intermediate probability of 0.1 allowed the algorithm to converge in the shortest time and with the smallest total sample size. The effect of using $p_0 = 0.2$ was similar to that of having a high y_t, i.e., given the intermediate probability, the cut-off on the ordered results list is lower. This makes it harder for y^* to achieve y_t, which makes for a longer $v = v - 1$ reverse search cycle. As for the lower value, 0.05, the resulting additional computing time would only be justifiable if the target p_f was lower than 10^{-4}. Concerning the complementary CDF comparisons in Fig. 7, it is noticed that the simulation with p_0=0.2 corresponds to a larger deviation when compared to the Monte Carlo assessments. Conversely, the same trends are closer for p_0=0.2, albeit at a higher computational cost.

p_0	0.05	0.1	0.2
time (h)	2:49	1:48	2:37
n_S	2700	2200	3700
v_{crit} (km/h)	264	263	265

Table 2: Variation of the intermediate probability p_0 (HSLM-A3, $y_t = 3.0$ m/s^2, $N = 100$).

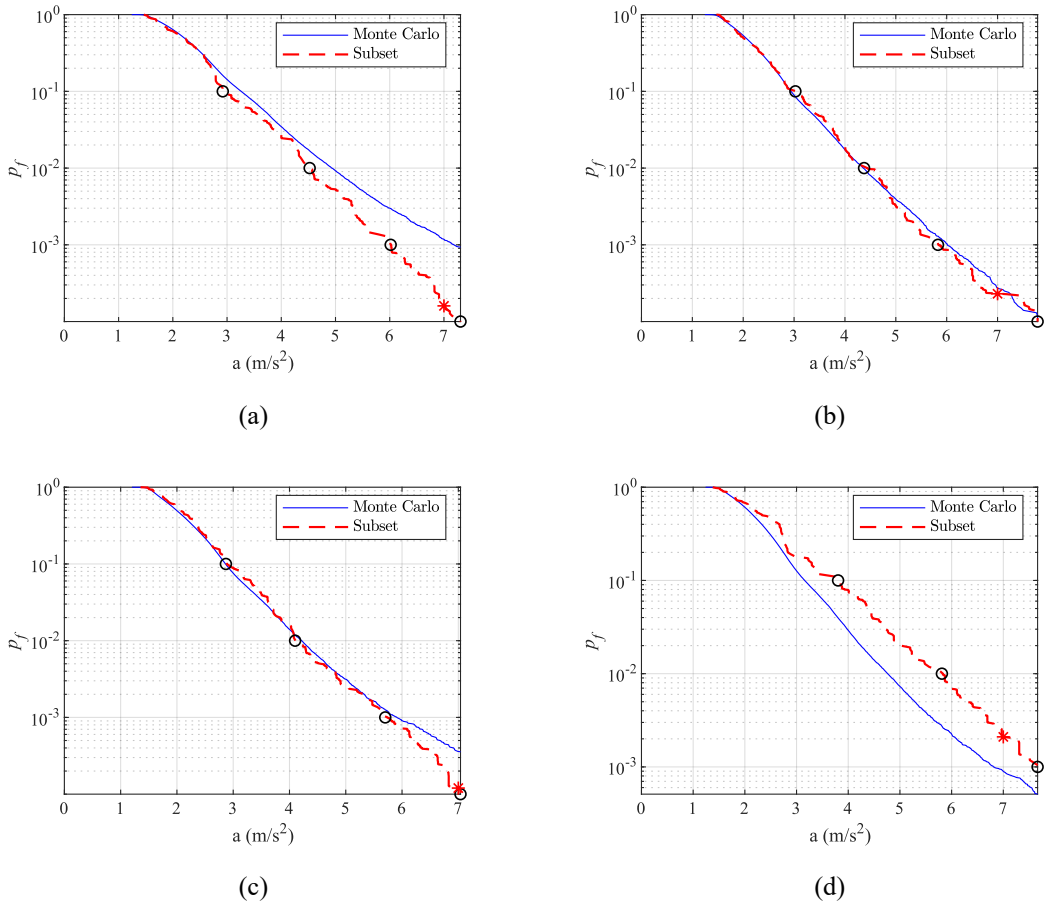

Figure 6: Complementary CDF of the subset simulations (HSLM-A3, $p_0 = 0.1$, $N = 100$) and corresponding Monte Carlo simulations with $N = 100000$. (c) y_t=3.0 m/s^2, v_{crit}=263 km/h; (d) y_t=3.5 m/s^2, v_{crit}=267 km/h.

Regarding the sample size, the comparison of N between 50, 100, 150 and 200 is calculated with fixed $y_t = 3.0$ and $p_f = 0.1$. As expected, Table 3 reveals that it takes more time to compute larger sample sizes, while the smallest size, 50, corresponds to the least amount of time and smallest total sample size. However, with an intermediate probability of 0.1, each level of a subset simulation with $N = 50$ provides only 5 elements to generate the samples of the following level. As a result, the number of failed candidate states in the MMA increases, introducing inefficacy when scaling the method by artificially limiting the dispersion of the results. Observing the complementary CDFs in Fig. 8, it is worth noting that there is an increased unevenness for $N = 50$, even if the resulting critical speed is the same as for $N = 100$. The larger sample sizes of $N = 150$ and $N = 200$ lead to similar results while consuming more computation time.

Given that the various applications lead to v_{crit} in close proximity, the final adopted values are $y_t = 3.0$m/s^2, $p_0 = 0.1$, and $N = 100$. Running the optimized algorithm

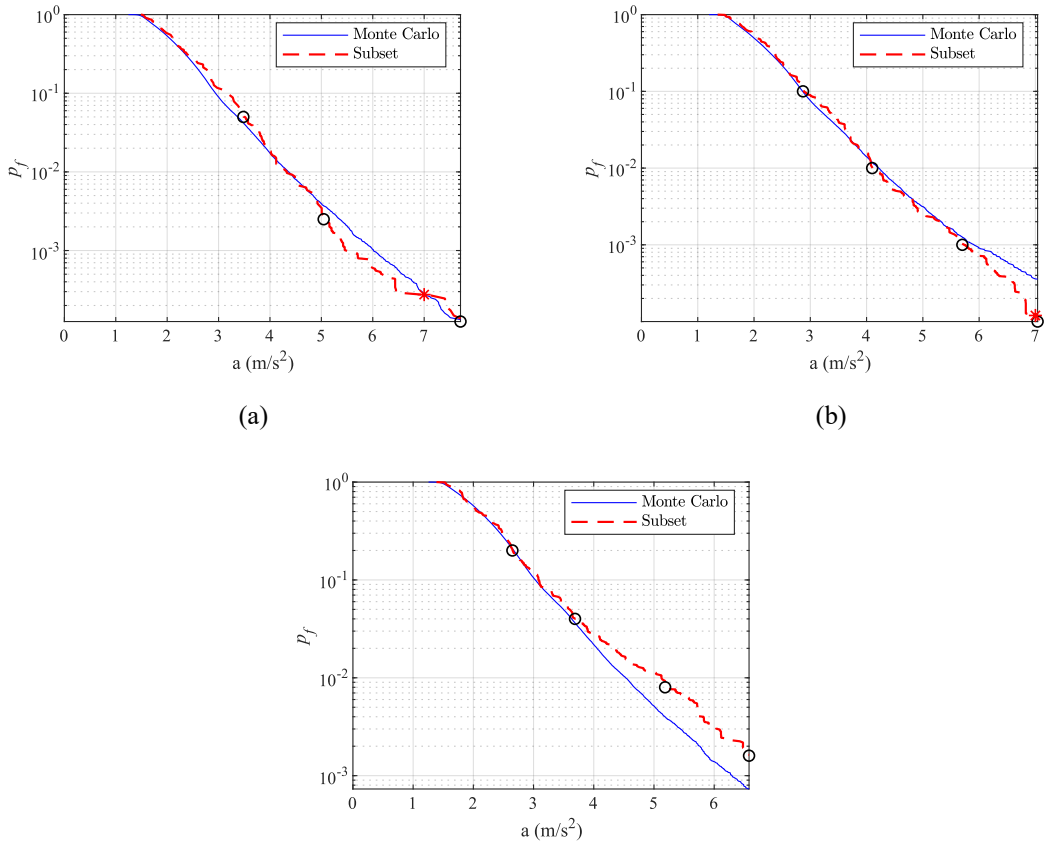

Figure 7: Complementary CDF of the subset simulations (HSLM-A3, $y_t = 3.0$ m/s^2, $N = 100$) and corresponding Monte Carlo simulations with $N = 100000$. (a) p_0=0.05, v_{crit}=264 km/h; (b) p_0=0.1, v_{crit}=263 km/h; (c) p_0=0.2, v_{crit}=265 km/h.

N	50	100	150	200
time (h)	1:01	1:48	3:26	2:52
n_S	1050	2200	6200	4000
v_{crit} (km/h)	263	263	267	265

Table 3: Variation of the sample size N (HSLM-A3, $y_t = 3.0$, $p_0 = 0.1$).

for the 10 HSLM-A trains results in the $v_{crit,i}$ listed in Table 4, which indicates that the critical speed for the Canelas bridge is 263 km/h.

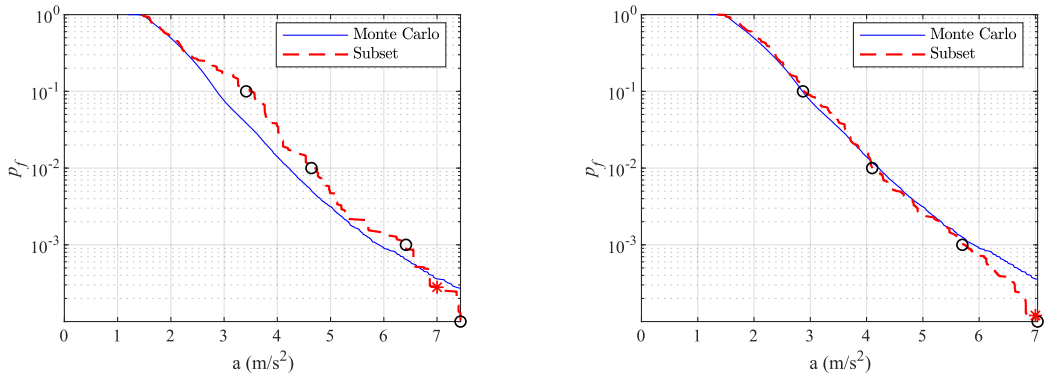

(a) (b)

Figure 8: Complementary CDF of the subset simulations (HSLM-A3, $y_t = 3.0$ m/s^2, p_0=0.1) and corresponding Monte Carlo simulations with $N = 100000$. (a) N=50, v_{crit}=263 km/h; (b) N=100, v_{crit}=263 km/h.

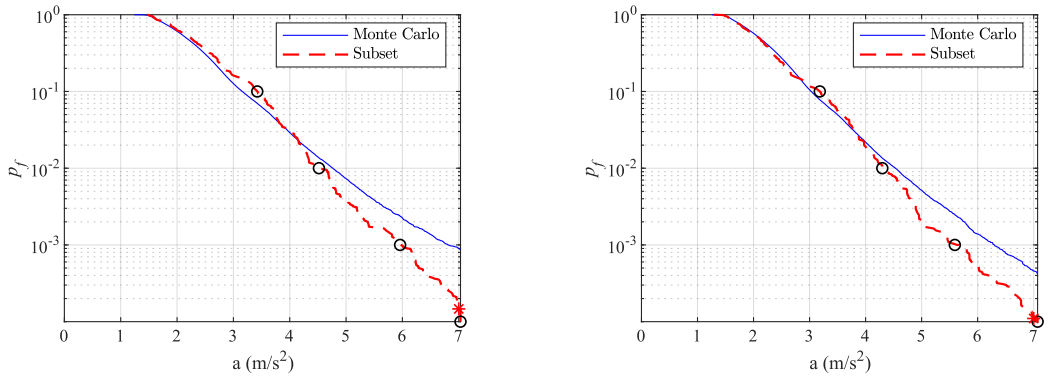

(c) (d)

Figure 8: (continued) Complementary CDF of the subset simulations (HSLM-A3, $y_t = 3.0$ m/s^2, p_0=0.1) and corresponding Monte Carlo simulations with $N = 100000$. (c) N=150, v_{crit}=267 km/h; (c) N=200, v_{crit}=265 km/h.

HSLM	A1	A2	A3	A4	A5	A6	A7	A8	A9	A10
$v_{crit,i}$ (km/h)	414	361	263	274	284	293	298	314	316	325

Table 4: Critical speeds for every HSLM-A.

4 Conclusions & Contributions

The employment of subset simulation is key to an efficient assessment of structural safety, since low probabilities of failure are estimated in this work with sample sizes of 400, instead of the equivalent 100000 associated with traditional Monte Carlo simulation. The iterative nature of the presented algorithm allowed to determine critical speeds with 2200 models, which is three orders of magnitude less than the total equivalent Monte Carlo total from 5.

The proposed algorithm allows the evaluation of critical speeds in a timely manner, contributing towards the study of the acceleration limit in ballasted track bridges. Future studies in this matter should consider the physical limit as a random variable in the case of new experimental studies existing.

Acknowledgements

The authors would like to acknowledge the financial support of "InBridge4EU – Enhanced Interfaces and train categories for dynamic compatibility assessment of European railway bridges" project funded by the Europe's Rail Joint Undertaking under Horizon Europe research and innovation programme under grant agreement No. 101121765 (HORIZON-ER-JU-2022-ExplR-02). Views and opinions expressed are however those of the author(s) only and do not necessarily reflect those of the European Union or Europe's Rail Joint Undertaking. Neither the European Union nor the granting authority can be held responsible for them. The authors also acknowledge the financial support of the Portuguese Foundation for Science and Technology (FCT) through the PhD scholarship PD/BD/143007/2018, and Base Funding – UIBD/04708/2020 of the CONSTRUCT – Instituto de I&D em Estruturas e Construções – funded by national funds through FCT/MCTES (PIDDAC).

References

[1] CEN, "Eurocode - Basis of structural and geotechnical design," Commité European de Normalisation (CEN), Brussels, Belgium, EN 1990, 2023.

[2] ERRI D 214/RP 9, "Rail bridges for speeds $>$ 200 km/h, final report," European Rail Research Institute, Utrecht, The Netherlands, Tech. Rep., 1999.

[3] M. Zacher and M. Baeßler, "Dynamic behaviour of ballast on railway bridges," in *Dynamics of High–Speed Railway Bridges. Selected and Revised Papers from the Advanced Course on 'Dynamics of High–Speed Railway Bridges', Porto, Portugal, 20–23 September 2005*. CRC Press, 2008, pp. 125–142.

[4] European Union Agency for Railways, "ERA1193-TD-01-2022 - ERA technical note on work needed for closing TSI open

points on bridge dynamics," Valenciennes, France, 2022. [Online]. Available: https://rail-research.europa.eu:443/about-europes-rail/europes-rail-reference-documents/additional-technical-material/

[5] JCSS, "Probabilistic Model Code," Joint Commitee on Structural Safety (JCSS), JCSS-OSTL/DIA/VROU -10-11-2000, 2001. [Online]. Available: https://www.jcss-lc.org/jcss-probabilistic-model-code/

[6] J. M. Rocha, A. A. Henriques, and R. Calçada, "Probabilistic assessment of the train running safety on a short-span high-speed railway bridge," *Structure and Infrastructure Engineering*, vol. 12, no. 1, pp. 78–92, 2016. [Online]. Available: https://doi.org/10.1080/15732479.2014.995106

[7] R. Allahvirdizadeh, A. Andersson, and R. Karoumi, "Partial safety factor calibration using surrogate models: An application for running safety of ballasted high-speed railway bridges," *Probabilistic Engineering Mechanics*, vol. 75, p. 103569, 2024. [Online]. Available: https://www.sciencedirect.com/science/article/pii/S0266892023001583

[8] CEN, "Eurocode 1 - Actions on structures - Part 2: Traffic loads on bridges and other civil engineering works," Commité European de Normalisation (CEN), Brussels, Belgium, EN 1991-2, 2023.

[9] S.-K. Au and J. L. Beck, "Estimation of small failure probabilities in high dimensions by subset simulation," *Probabilistic Engineering Mechanics*, vol. 16, no. 4, pp. 263–277, 2001. [Online]. Available: https://www.sciencedirect.com/science/article/pii/S0266892001000194

[10] K. M. Zuev, "Subset Simulation Method for Rare Event Estimation: An Introduction," in *Encyclopedia of Earthquake Engineering*, M. Beer, I. A. Kougioumtzoglou, E. Patelli, and I. S.-K. Au, Eds. Heidelberg, Germany: Springer, 2013, pp. 1–25. [Online]. Available: https://doi.org/10.1007/978-3-642-36197-5_165-1

[11] MATLAB®, "Academic Research," The MathWorks Inc., Natick, Massachusetts, USA, 2018, release R2018a.

[12] ANSYS®, "Release 19.2," ANSYS Inc., Canonsburg, Pennsylvania, USA, 2018.

[13] G. Ferreira, P. Montenegro, J. R. Pinto, A. A. Henriques, and R. Calçada, "A discussion about the limitations of the Eurocode's high-speed load model for railway bridges," *Railway Engineering Science*, vol. 32, no. 2, pp. 211–228, 2024.

[14] F. Uribe, "Monte Carlo and subset simulation example," 2016. [Online]. Available: https://www.mathworks.com/matlabcentral/fileexchange/57947-monte-carlo-and-subset-simulation-example

[15] C. Bonifácio, D. Ribeiro, R. Calçada, and R. Delgado, "Calibration and validation of the numerical model of a short-span railway bridge based on dynamic tests," in *Proceedings of the 9th International Conference on Structural Dynamics*, Porto, Portugal, 2014.

[16] J. M. Rocha, "Probabilistic methodologies for the safety assessment of short span railway bridges for high-speed traffic," Doctoral Thesis, Faculdade de Engenharia da Universidade do Porto, Porto, Portugal, 2015. [Online]. Available: https://repositorio-aberto.up.pt/handle/10216/83809

[17] P. Bjerager, "Methods for Structural Reliability Computations," in *Reliability Problems: General Principles and Applications in Mechanics of Solids and Structures*, ser. International Centre for Mechanical Sciences, F. Casciati and J. B. Roberts, Eds. Vienna, Austria: Springer, 1991, pp. 89–135. [Online]. Available: https://doi.org/10.1007/978-3-7091-2616-5_3